RSC Advances

ROYAL SOCIETY OF CHEMISTRY

www.rsc.org/advances

Targeted and controlled drug delivery using a temperature and ultra-violet responsive liposome with excellent breast cancer suppression ability

Huafei Li[a, c, †], Cong Wu[b, †], Mao Xia[c, †], He Zhao[c], Mengxin Zhao[c], Jin Hou[b], Rong Li[b], Lixin Wei[a, *], Li Zhang[b, *]

[a] Tumor Immunology and Gene Therapy Center, Eastern Hepatobiliary Surgery Hospital affiliated to the Second Military Medical University, 225 Changhai Road, Shanghai 200433, China

[b] Department of Pharmacy/Laboratory Diagnosis, Changhai Hospital affiliated to the Second Military Medical University, 168 Changhai Road, Shanghai 200433, China

[c] International Joint Cancer Institute, the Second Military Medical University, 800 Xiangyin Road, Shanghai 200433, China

† These authors contributed equally to this work

* Correspondence:

Dr. Lixin Wei, Tumor Immunology and Gene Therapy Center, Eastern Hepatobiliary Surgery Hospital affiliated to the Second Military Medical University, 225 Changhai Road, Shanghai 200433, China, E-mail: lixinwei@summu.edu.cn

Dr. Li Zhang, Department of Pharmacy, Changhai Hospital affiliated to the Second Military Medical University, 168 Changhai Road, Shanghai 200433, China, E-mail: Zhanglicdma@189.cn

Abstract

Drug delivery system (DDS) with favorable serum stability, high intra-tumor accumulation and tumor specific drug release are highly desired for promoting chemotherapeutic efficacy. However, more stable of a DDS means more difficult to release its content, and vice versa. In order for resolving this conflict, a Fab conjugated thermo-responsive liposome (FCTRL) based on 1,2-bis(10,12-tricosadiynoyl)-sn-glycero-3-phosphocholine (DC8,9PC) and PID_{118}-b-PLA_{71} diblock copolymer (PPDC) was developed in this study. DC8,9PC is a type of phospholipid, which can form intermolecular cross-linking within the liposomal bilayer by Ultra-Violet irradiation, contributing to superior serum stability in the blood vessels. While PPDC is a thermo-responsive block copolymer, which demonstrates temperature controlled ON-OFF drug release with a volume phase transition temperature (VPTT) of approximately 38.5℃. The well modified FCTRLs are of desired particle size, drug loading content and drug release profile. The surface morphology and pharmacokinetics were also characterized. The cellular uptake and intracellular accumulation of FCTRL are significantly promoted by its proper size, temperature regulated passive and Fab navigated active targeting. With the co-operation of all the above superiorities, the FCTRL DDS demonstrates exceptionally excellent tumor suppression abilities against breast cancer in both *in* and *ex vivo* experiments, which merits further investigation in the clinic.

Key words: breast cancer, nanomedicine, thermoresponsive, ultra-violet irradiation polymerizing, immunoliposomes, pharmacokinetics

Introduction

Chemotherapy has been widely used against many malignancies.[1] The ideal goal of chemotherapy is to deliver high-efficacy drugs at the right time to the right location at the right concentration over the right length of time [2]. However, this pharmacokinetic sweet spot can hardly be achieved due to the distinctly different transient states of drugs in adhesion, distribution, metabolism and excretion (ADME).[2] The clinical application of a variety of anti-cancer drugs is limited due to the serious side-effects against normal tissues because of systemic administration [3-5]. Moreover, cancer cells tend to develop drug resistance, especially multidrug resistance (MDR), during the prolonged course of chemotherapy, characterized by cancer progression or recurrence.[2, 6] Thus, developing novel strategies for adequate and specific delivery of antineoplastic agents to tumor tissues and cells is important for enhanced chemotherapeutic index.

Anti-cancer drug delivery to malignant cells in solid tumors involves three processes, 1) transport through blood circulation to tumor vessels, 2) transport across vasculature walls into surrounding tumor tissues, 3) transport through tumor interstitial space to malignant cells. These processes are determined by the physicochemical properties of drugs and the biologic properties of tumor microenvironment, some of which are distinct from normal tissues.[3, 7] With the development of material science and nanotechnology, nanoparticles based drug delivery systems (DDS) offer new hopes for improving the efficiency of chemotherapy with the following potential advantages: Firstly, nanoparticles with desired size (e.g., 100–200 nm in diameter) could escape from the reticuloendothelial system (RES) to realize a favorable *in vivo* stability in the circulating blood [8]. Secondly, nanomedicine could allow the encapsulated drugs to accumulate in tumor tissues via the enhanced permeability and retention (EPR) effect and minimize the systematic toxicity.[9, 10] Thirdly, nanoparticles decorated with various ligands, such as monoclonal antibodies (mAbs), can realize targeted delivery and thus enhance internalization of encapsulated agents into tumor cells via endocytosis.[2, 5, 11]

Finally, nanoparticles are not physically recognized as substrates by the ATP-binding cassette (ABC) efflux pumps, which are proved to be overexpressed on chemo-resistant cancer cells and can extrude toxins from cells, conferring MDR to a broad spectrum of cytotoxic agents.[12, 13]

Up to now, two representative nanomedicines, Doxil and Abraxane, have been approved by the U.S. Food and Drug Administration (FDA).[14, 15] Also, many novel nanomedicine formulations based on polymeric nanoparticles, micelles, liposomes et al. have been extensively investigated recently for their effectiveness in diagnosing and treating malignancies.[14, 15] Currently, increasing researches are focusing on improving the stability of the DDS in blood vessels and facilitating the release of encapsulated drugs in tumor issues and cells.[2, 5, 16-18] However, it seems that more stable of a DDS means more difficult to release its content at the vicinity of tumors, and vice versa.[16-20] The contradiction between particle stability and drug release remains a key point to resolve for further improving the tumor suppressing activities.

Herein, we constructed a Fab conjugated temperature responsive liposome (FCTRL) based on 1,2-bis(10,12-tricosadiynoyl)-sn-glycero-3-phosphocholine (DC8,9PC) and PID_{118}-b-PLA_{71} diblock copolymer (PPDC). DC8,9PC is a type of phospholipid, which can form intermolecular cross-linking through the diacetylenic group to produce a conjugated polymer within the hydrocarbon region of the bilayer by Ultra-Violet (UV) irradiation (Figure 1b and d).[5, 21] The DC8,9PC based liposomes exhibit pleasurable serum stability after UV irradiation in our previous study.[5] PPDC is a thermo-responsive block copolymer. The PPDC based Fab conjugated immunomicelles demonstrated tumor specific drug release and subsequent controlled expression of *in vitro* and *in vivo* cytotoxicity against gastric cancer cells with applied temperature changes in our previous work.[16] In this study, the FCTRL based on the self-assembling of DC8,9PC and PPDC not only exhibits outstanding serum stability and prolonged circulation time in the circulating blood, but also demonstrates temperature controlled ON-OFF drug release with a proper

volume phase transition temperature (VPTT) of approximately 38.5℃. What's more, with the surface decoration of Trastuzumab Fab fragments, the intra-tumor accumulation and intracellular uptake of FCTRL was further improved. The *in and ex vivo* experimental results reveal that drug-loading FCTRL exhibits exceptional excellent tumor suppressing ability against Her-2 (human epidermal growth factor receptor-2) positive breast cancers, which merits further investigation in the clinic.

Materials and methods

Materials

DC8,9PC and 1,2-distearoyl-sn-glycero-3-phosphoethanolamine-N-[maleimide(polyethylene glycol)-2000] (Mal-PEG) were purchased from Avanti Polar Lipids (Pennsylvania, USA). PPDC was synthesized as described in our previous study (Figure 1a).[16] Chemotherapeutic drug 5-fluorouracil (5-Fu) was obtained from Melonepharma CO. LTD (Dalian, China). The CdSe/ZnS core-shell type quantum dots (Qds) and Fluorescein Isothiocyanate (FITC) were purchased from Sigma-Aldrich (St. Louis, USA). Trastuzumab (Trade name: Herceptin) was purchased from Roche Pharma Ltd. (Basel, Switzerland). The Alexa Fluor 488 labeled Goat anti-human secondary antibody was obtained from Life Technologies Corporation (California, USA).

Fabrication of FCTRL (Figure 1b)

PC liposomes, composed of DC8,9PC, PPDC and mal-PEG were prepared by the thin-film hydration method as previous descriptions with minor modifications.[5, 21] Briefly, 2.0mg DC8,9PC, 0.2mg mal-PEG and 0.8mg PPDC were dissolved in 800μl mixed solvent of chloroform and methyl alcohol with the volume ratio of 1:1. After complete dissolution, the solvent was removed in a rotary evaporator under vacuum and flashed with nitrogen to obtain a thin lipid film, which was re-suspended in 2ml of 5-Fu solution (0.5mg/mL in PBS) until completely hydrated to obtain a 5-FU loaded liposome suspension. Then, the liposome suspension was serially passed through 0.8, 0.4 and finally 0.2μm polycarbonate membranes (Avestin, Canada). Un-encapsulated 5-FU was removed by dialysis (Molecule weight cut-off, MWCO: 3kDa) at 4℃ overnight. The resulting liposome suspensions were stored at 4℃ for future usage. The empty and Qds loaded liposomes were prepared in the same way except for washing out by respectively PBS buffer or Qds solution instead. After Trastuzumab and Bovine Serum Albumin (BSA) being thiolated by

dithiotheritol as described in our previous publications,[5, 16] the resulting Trastuzumab~SH and BSA~SH fragments were respectively conjugated onto the liposomal surface via the reaction between the ~SH and Mal-group at 4℃ and N_2 environment overnight. The pH of the reaction mixture was adjusted to 8.4 by using sodium borate buffer. The un-conjugated fragments were removed by dialysis (MWCO: 100kDa). For UV irradiation, liposomal solutions were exposed to 20 irradiation cycles at 4℃, with a 254nm UV light dose of 360mJ/cm^2 per cycle using a Stratalinker-UV 1800.[5, 10]

Size distribution and morphology

The liposomal size distribution was determined by ZetaSizer (Nano-ZS, Malvern Instruments, Worcestershire, UK). To prepare stained specimens for transmission electron microscopy (TEM, Hitachi, H-7000 Electron Microscope) experiments, 5µl liposomal suspension was dropped on 200-mesh Formvar-free carbon-coated copper grids. After the water evaporating by exposing to air at room temperature (RT), the sample was inversely covered on a drop of 2% hydrodated phosphotungstate (PTA). The TEM images were obtained at 100 kV.

Temperature responsive properties

UV (UVeVIS spectrometer, Cary-100, Varian) fitted with temperature and a stirring controller was used to monitor the sample absorption profile at 300 nm. The incident light passes through the center of sample cell fitted with a thermometer. The VPTT was defined at the absorption of the liposomal suspension sharply increased to 50%.[16]

Surface binding to Her-2 antigen

The FCTRL binding to surface Her-2 antigen was assessed by confocal laser scattering microscopy (CLSM). Briefly, harvested Her-2 positive MDA-MB-231cells were placed onto poly-D-lysine (sigma-Aldrich) coated microscope

slides. Samples were fixed by 4% paraformaldehyde and successively incubated with FCTRL and Alexa-Fluor 488 labeled Goat-anti-human secondary antibodies for 1 hour in room temperature (RT), respectively. The green color surrounding the cells indicates the successfully binding of Fab fragments (on liposomal surface) to Her-2 antigen (on cell surface), which was observed by CLSM (Olympus FV1000) in both 2D and 3D models.

Drug releasing profile

For 5-Fu releasing profile determination, a dialysis bag (MWCO: 3kDa) containing 3ml irrad or non-irrad liposomal 5-Fu was respectively put into a beaker with 500ml PBS. The beaker was fixed in a water bath respectively kept at 37 and 40℃ with continues siring. At different time intervals, approximately 500μl solution outside the dialysis bag was sampled and measured by High Performance Liquid Chromatography (HPLC) to determine the 5-Fu concentration following previous studies.[22, 23] The cumulative drug release was calculated by the following equation:

$$\text{Cumulative release} = \frac{C_{\text{Outside dialysis bag}} \times 500\text{ml}}{C_{\text{Inside dialysis bag}} \times 3\text{ml}} \times 100\%$$

Serum stability evaluation by DLS

A BSA solution in dulbecco's modified eagle medium (DMEM, GIBCO, Life Technologies, California, USA) with a concentration of 50% (m/v) was used as an *in vitro* serum model to mimic the *in vivo* status. Then the irrad and non-irrad liposomes were separately mixed with the serum model at 37℃ for 24 hours. The dynamic light scattering (DLS) was used to measure the size distribution profile of BSA/Liposome mixture after different time intervals, respectively.

Cell culture

Two Her-2 positive human B breast cancer cell lines, MDA-MB-231 and MCF-7, were obtained from the American

Type Culture Collection (ATCC). Cells were propagated and maintained in DMEM supplemented with 10% (v/v) fetal bovine serum (FBS, GIBCO, Life Technologies, California, USA) in a controlled atmosphere incubator at 37°C with 5% CO_2.

Biocompatibility evaluation

MDA-MB-231 cells (3.0×10^3) were seeded into a 96-well microplate and cultured overnight. Then cells were incubated with empty FCTRLs and BCTRLs (BSA conjugated temperature responsive liposomes) over a range of concentrations from 1 to 64 μg/mL in DMEM/FBS at 37℃/40℃. After 48 hours, samples were washed and incubated with 10% Cell Counting Kit-8 (CCK-8, Beyotime Institute of Biotechnology, Shanghai, China) for 2 hours protected from light. The absorbance (Ab) at 450nm was recorded by a micro-plate reader (Thermo Multiskan MK3, Thermo Scientifc) and cell viability was calculated as the following equation:

$$\text{Cell viability}\% = \frac{(\text{Ab}_{\text{Sample}} - \text{Ab}_{\text{Blank}})}{(\text{Ab}_{\text{Control}} - \text{Ab}_{\text{Blank}})} \times 100\%$$

where Ab_{sample} represents absorbance of test well, $Ab_{control}$ represents absorbance of positive growth control well (incubated without any additional substances at each temperature), and Ab_{blank} represents absorbance of only CCK-8.

Cellular uptake and internalization

Cells were seeded into a 48-well microplate (1×10^5 cells) and incubated with 1μg/mL free and liposomal Qds in DMEM/FBS at 37 and 40℃ for 4h. Cells incubated with culture medium were used as a negative control. After washing, a FACScan Flow Cytometer (Becton Dickinson, San Jose, CA) was used to assess the cellular uptake of Qds by detecting the mean fluorescence intensity (MFI) of FL-2. Additionally, each sample was also visualized using an inverse fluorescent microscope.

Animals

Four-week-old female BAL B/C nude mice and ICR mice were purchased from Shanghai Experimental Animal Center of Chinese Academic of Sciences (Shanghai, China), housed in specific pathogen-free conditions and treated in accordance with guidelines of the Committee on Animals of the Second Military Medical University (Shanghai China).

Pharmacokinetics and *in vivo* distribution analysis

The pharmacokinetics (PKs) and *in vivo* distribution analysis was done following *Joseph M. Tuscano*'s study with minor revisions.[24] Briefly, 8-week-old ICR mice were randomly administrated tail vein injection of free or liposomal FITC at a dosage of 5mg/kg. Then 10μl of blood were collected through tail vein nicking from each mouse at different time intervals. Samples were immediately diluted into 250μl of 0.5mmol/L EDTA-PBS, followed by a centrifugation (300g×5min). Plasma FITC was extracted by acidified isopropanol (75mmol/L hydrochloric acid in 90% isopropanol) at 4°C for 20h. The FITC concentrations were determined by measuring the fluorescence intensity at 488/520nm (excitation/emission) and expressed as μg/mL (FITC/blood plasma). The data were analyzed by the PK solver software.[25] For biodistribution assays, tumor bearing mice were randomly administrated tail vein injection of free and liposomal FITC at a dosage of 5mg/kg (n=3 mice per treatment). Mice were sacrificed 24h after treatment and part of tumor, heart, liver, spleen and kidneys were removed, washed, weighed, and single-cell suspensions were made. FITC was extracted from cells and the concentrations (expressed as μg/g tissue) were determined as described above. What's more, part of the tumor tissues were collected and subjected to frozen sections, which were detected by a CLSM.

***In vivo* anti-tumor activity assessment**

MDA-MB-231 and MCF-7 cells (1×10^7) in 100μl of PBS buffer were inoculated subcutaneously into the lateral flank of 6-week-old BAL B/C nude mice. When tumors reached about 50-60mm^3 in volume, the inoculated mice were randomly assigned to 4 groups with 4 each for the treatment of PBS, free and liposomal (FCTRL and BCTRL) 5-Fu (5mg/kg) via the tail vein weekly for 3 times. Post-operation monitoring was exercised at least once a day and the tumor size was measured in two perpendicular diameters with precision calipers and calculated in a range of 60 days. The tumor volume was measured according to the following equation:

$$\text{Tumor volume} = \text{Length} \times \text{Width}^2/2 \quad [26]$$

where length and width refers to the longest and the shortest diameters of tumors, respectively.

Statistical analysis

Statistical analysis was performed by Student's unpaired *t* test or one-way ANOVA to identify significant differences unless otherwise indicated. Differences were considered significant at a p value of less than 0.05.

Results and discussion

Size distribution and morphology

Figure 1c indicates that a ~32% decrease of liposomal radius was occurred after UV irradiation (from approximately 138.81nm of non-irrad FCTRL to 94.39nm of irrad FCTRL). We ascribe this interesting physical change to the inter-molecular cross-link of DC8,9PC in the liposomal bilayers as a result of UV irradiation polymerizing (Figure 1d), which was validated in our and other's previous studies [5, 21]. The TEM results (Figure 1f) suggest that FCTRL demonstrates a regular spherical core-shell morphology at 37℃ (T<VPTT). The well modified core-shell structure and proper size distribution make our immunoliposome an ideal drug delivery system for chemotherapeutic agents.

Thermo-responsive property

Poly(N-isopropylacrylamide) (PNIPAM) is a well-known thermoresponsive polymer with a lower critical solution temperature (LCST) around 32℃, which can be regulated by hydrophilic or hydrophobic modification.[27] It should be mentioned that the UV was always used to detect the transmittance of PNIPAM based copolymer solution, in such case, the temperature at the phase transition should be named as volume phase transition temperature (VPTT) instead of LCST.[16] Besides, surface functional groups may have remarkable influence on the VPTT of nanoparticles [27].

It is well established that the high metabolism of tumor cells requires much more oxygen, nutrients, gas exchange and waste removal, while the heterogeneous structure and distribution of the tumor blood vessels slows down the energy exchanging between intra- and extra-tumor. All these result in relatively higher temperature in tumor tissues than that in normal tissues [28-30]. Thus, the most suitable VPTT of an ideal drug delivery system might be approximately 38~39℃, which lies between normal body temperature (36~37℃) and tumor temperature (approximately 40℃). In order to tune the liposomal VPTT to this suitable temperature, FCTRLs were prepared by mixing DC8,9PC, mal-PEG

and PPDC at a mass ratio of 2:0.2:0.8 based on our preliminary experimental results (data not shown). The liposomal thermoresponsive behavior in PBS was investigated with the results showing in Figure 1e. As we can see, the FCTRL exhibits a VPTT of approximately 38.5℃. The results were confirmed by TEM (Figure 1f), of which the results revealed that the well modified core-shell structure of FCTRL was disrupted by increasing the local temperature to 40℃ (T>VPTT). It is helpful to know that the thermos-responsive segments (PID chain) will change from hydrophilic to hydrophobic as T > VPTT. This hydrophilic/hydrophobic transition enhanced the hydrophobicity of the block copolymer on liposomal surface. Such hydrophobicity increase leaded to the inter-liposome aggregation and/or the disruption of liposomal compartment (Figure 1f, and Supplementary Figure 2)[16, 31, 32], resulting in temperature controlled ON-OFF drug release which we will discuss later (Figure 2b).

Fab fragments loading

The successful anchoring of Fab fragments on liposomal surface was confirmed by CLSM. After the Her-2 positive MDA-MB-231 cells were successively incubated with FCTRL and Alexa-Fluor 488 labeled Goat-anti-human secondary antibodies, the cell morphology was observed by CLSM. The green color surrounding the cells was obviously observed in both 2D and 3D models (Figure 2a), which directly indicated the existence of Fab fragments in the liposomal DDS.

Drug loading/releasing profile

In was well expected that FCTRL could be an excellent drug carrier benefits from the stable structure. For the validation of this expectation, we firstly evaluated the 5-Fu loading content (LC) of FCTRL according to the following function: $\mathrm{LC}\ (\%) = \frac{C_{5-Fu}}{C_{polymer}} \times 100\%$. The results revealed a relative high LC of 16.2% with our immunoliposomes.

The drug release profiles were determined in PBS buffer respectively at 37 and 40℃ with the results showing in Figure 2b. As we can see, both the irrad and non-irrad liposomes exhibit similar and sustained release of containing drugs at 37℃ (T<VPTT) with no initial burst during the period of 48 hours. Because of PC polymerization in liposomal bilayer, slower drug release was observed with the irrad liposomes than with the non-irrad ones. By contrast, relatively rapid release of containing drugs from both irrad and non-irrad liposomes was observed at 40℃ (T>VPTT), with more than 50% and approximately 80% encapsulated 5-Fu being released after 8 and 24 hours, respectively. The temperature triggered drug release can be attributed to the grafting of thermos-responsive polymers (PPDC) on liposomal surface. The PPDC displays a hydrophilic head on exterior and interior surface of liposomal bilayers (left panel of Supplementary Figure 2). When the temperature increased to T>VPTT, the PID chains will change from hydrophilic to hydrophobic. Then they will interact with the lipid bilayer inducing aggregation and destabilization, resulting in release of entrapped drugs (right panel of Supplementary Figure 2)[32-34].

Favorable biocompatibility

As indicated in Figure 2c, both the empty FCTRL and BCTRL demonstrate low-cytotoxicity to MDA-MB-231 cells in concentrations of up to 64μg/mL at both temperatures (37 and 40℃). It is worth mentioning that the cell viability of FCTRL incubated cells had a little decrease compared with BCTRL incubated cells, which may be related with the tumor suppression effect of Fab fragments.

Serum stability

Considering the intended use (intravenous administration), the DMEM containing 50% FBS was employed as an *in vitro* serum model to check the liposomal serum stability following previous publications.[16, 35] The existence of FBS was employed to mimic a variety of serum proteins in the complicated environment within the blood vessels. Table 1

shows the particle size and Polydispersity index (PDI) of irrad and non-irrad liposomes after incubation with DMEM/FBS for different time intervals. As we can see, after a 24-hour-incubation, the particle radius of non-irrad liposomes was altered from 130.17±24.76nm to 187.34±59.82 nm, compared with that of irrad liposomes from 93.74±15.33nm to 102.55±22.7. The PDI of non-irrad liposome was increased from 0.036 to 0.102, compared with that of irrad liposomes from 0.027 to 0.050. The fewer variations of size distribution and PDI suggest that the immunoliposome owns higher stability after UV irradiation, which can also be ascribed to the PC polymerization in liposomal bilayer.

Intracellular uptake

Effects of temperature and Fab decoration on intracellular uptake of the liposomes were investigated by FCM and CLSM using Qds-labeled FCTRLs and BCTRLs. Figure 3b and 3d demonstrate that the red fluorescence derived from free Qds incubated cells was negligible at both 37 and 40°C. The BCTRL and FCTRL significantly enhanced the intracellular uptake of encapsulated Qds indicated by the increased MFI of FL-2 (red fluorescence). In addition, the Fab fragments decoration can significantly enhance the intracellular uptake of encapsulated Qds at the same incubation temperature, which was approximately 1.4 and 1.55 times that of BCTRL/Qds incubated MDA-MB-231 and MCF-7 cells, respectively. We further investigated the temperature-modulated intracellular uptake. As we can see from Figure 3b and 3d, the fluorescence from Qds inside the cells was clearly improved above the VPTT (40°C) for both the FCTRLs and BCTRLs. The FCM results were validated by CLSM as displayed in Figure 3a and 3c.

It should be noted here that, firstly, the liposomes showed obvious enhancement for the intracellular uptake of encapsulated agents similar to our previous studies [5, 20]. Secondly, the intracellular uptake was significantly enhanced by the active targeting via antibody-antigen identification and combination. More importantly, upon temperature increasing above the VPTT, the corona-forming polymer chains collapse with the dehydration of IPAAm units.

Because of significant polymer conformational changes, hydrophobic interactions between the liposomes and cell membranes increase.[27, 37] Consequently, adhesion of the liposomes to the cell surfaces was promoted, followed by further enhancement of intracellular uptake.

***In vitro* cytotoxicity**

Figure 4 illustrates the cell viability of Her-2 positive MDA-MB-231 and MCF-7 cell lines treated with 5-Fu loading liposomes with and without Fab conjugation, which was accessed in comparison with that of free 5-Fu at the various drug concentrations and time intervals at 37 and 40℃. As illustrated in Figure 4a and d, both MDA-MB-231 and MCF-7 cells showed a significantly lower cell viability after the treatment of liposomal drugs than free drugs, while FCTRL/5-Fu exhibited more potent tumor suppressing activity compared with BCTRL/5-Fu in all the tested concentrations at both temperatures due to the intracellular drug accumulation enhanced by liposomes and Fab fragments. Similarly, for the liposomal drugs, the cell viability as incubated at 40℃(T > VPTT) was lower than that at 37℃(T < VPTT) because the temperature promoting intracellular uptaking and drug releasing. Similar results were obtained when cells were incubated with free and liposomal 5-Fu (0.525μg/ml) at different time intervals from 0-72 hours (Figure 4b and e). Furthermore, the half maximal (50%) inhibitory concentration (IC50) of 5-Fu was calculated to evaluate the cytotoxicity of the liposomal drug delivery systems according to the 5-Fu concentration dependence of the cell viability profile. It was shown in Figure 4c and f that FCTRL/5-Fu demonstrated the lowest IC50 to both MDA-MB-231 (0.09±0.019μg/mL) and MCF-7 (0.09±0.025μg/mL) cells at 40℃ (T>VPTT), which was about 8 times lower than that of free drugs. These results further confirmed that both the temperature and Fab decoration successfully enhanced the liposomal cytotoxicity against HER-2 positive breast cancer cells.

Pharmacokinetics

After a short injection of free and liposomal 5-Fu at 5mg/kg healthy to ICR mice, the plasma drug concentrations were measured by HPLC at different time intervals. The data were analyzed using the PK solver software [23, 25], and the results are all fitted to a trilocular pattern [5, 37]. The time-concentration curve is shown in Supplementary Figure 1 and the PK parameters in Table 2. As we can see, a remarkable difference in plasma pharmacokinetics was observed after the tail vein administration of free and liposomal 5-Fu. The $t_{1/2\gamma}$ (the elimination half time in the elimination phase) was relatively longer for irrad FCTRLs (34.59±1.29 h) than that for non-irrad liposomes (21.63±0.60 h) and free drugs (8,63±3.83 h). In accordance, the clearance (CL) was significantly reduced for irrad liposomes (0.65±0.07 ml/h versus $CL_{\text{non-irrad liposomes}}$: 1.47±0.10 ml/h, $CL_{\text{free 5-Fu}}$: 9.74±1.71ml/h). As we can see, liposomal drugs owned a longer circulation time in the blood vessels. Also, the circulation time was further prolonged by higher serum stability as a result of inter-molecule cross-link in the liposomal bilayers, which we have discussed above.

***In vivo* distribution and tumor accumulation assays**

In order for *in vivo* distribution and tumor accumulation assays, tumor bearing BAL B/C nude mice were injected with free and liposomal FITC via tail vein. Twenty-four hours later, tissues were harvested and the sum total FITC was extracted and measured. Figure 5b demonstrated that there was a significant increase in tumor FITC accumulation in FCTRL/FITC treated mice compared with BCTRL/FITC (*p=0.039) and free FITC treated ones (**p=0.000). The heart, liver and spleen all showed less FITC accumulation with liposomal FITC injection than with free FITC treatment (*p<0.05). There was no difference in FITC accumulation among treatments for the kidneys (p=0.33). The displayed fluorescent image of different frozen sections (Figure 5a) also demonstrated significantly higher green fluorescence in tumor tissues of mice treated with liposomal FITC than with free FITC. Moreover, the

intra-tumor accumulation of FCTRLs was much higher than that of BCTRLs. The intermolecular cross-linking in the liposomal bilayer as a result of UV irradiation increased the *in vivo* stability and prolonged its circulation time in the blood vessels. This is of great importance for tumor accumulation. As the liposomal drug delivery system arriving at the tumor site, both the passive targeting via EPR effect and active targeting via antibody-antigen reaction promoted the relatively specific intratumor accumulation. Additionally, it was reported that the temperature of some solid tumor was 1.5~3℃ higher than that of normal tissue [5, 37]. While the VPTT of the liposomes was about 38.5℃, which indicated that part of the liposomal surface will transfer from hydrophilic to hydrophobic in the tumor tissues and cells. This phase transition can improve intracellular uptake which we have discussed above. On the other hand, such temperature regulated passive targeting could be very useful in conjunction with local heating cancer therapy.

***In vivo* tumor suppression**

For the evaluation of *in vivo* anti-tumor activities, MDA-MB-231 and MCF-7 cells were inoculated subcutaneously into the right flank of BAL B/C nude mice. When the tumors reached about 50-60mm^3 in volume, mice were randomly treated with free and liposomal 5-Fu (5mg/kg). The relative tumor volume was calculated and illustrated in Figure 5c-d. As we can see, mice treated with liposomal 5-Fu demonstrate a remarkable decrease in tumor burden compared with free 5-Fu and PBS treatment as measured by tumor volume. Otherwise, FCTRL/5-Fu exhibits a more outstanding tumor suppression ability in both breast cancer cell lines comparing with BCTRL/5-Fu, with respectively 1/5 (MDA-MB-231) and 3/5 (MCF-7) mice of complete remission (CR) indicated by no measurable mass. In our opinion, this exceptional excellent *in vivo* anti-tumor activity is the co-operative action of the following effects: (1) enhanced intracellular uptake due to effective endocytosis based on well-defined liposomal structure and size distribution; (2) enhanced serum stability as a result of UV irradiation polymerizing can contribute to long circulation time and durable anti-tumor activity; (3) enhanced tumor accumulation and retention *in vivo* through dual targeting

function: passive targeting through EPR effects and active targeting through antigen-antibody reaction. (4) Relative high temperature (T>VPTT) could result in phase transition of liposomal surface PPDC from hydrophilic to hydrophobic, which can increase the hydrophobic interactions between the liposomes and cell membranes. Thus, the adhesion and following intracellular uptake of the liposomes was promoted. More importantly, this phase transition can ultimately promote the release of encapsulated drugs. This temperature controlled ON-OFF drug release at the vicinity of cancer tissues or inner cancer cells can finally contribute to sufficient and efficient local drug concentration, resulting in exceptional potent tumor suppression abilities.

Conclusions

In this study, we developed a drug delivery system of 5-Fu-loaded Fab conjugated thermoresponsive liposomes (denoted as FCTRL) for sustainable & targeted delivery and temperature controlled ON-OFF release of chemotherapeutic agents as a model drug for treatment of Her-2 positive breast cancer cells. The VPTT of the immunoliposome is tuned to an ideal temperature of approximately 38.5℃, which is between the temperatures of normal and malignant tissues. The liposomal properties, including the size distribution, well modified core-shell structure, thermoresponsive characterization and favorable biocompatibility, were clearly demonstrated. The effects of UV irradiation, temperature and Fab targeting on drug loading & releasing, serum stability, intracellular uptake, pharmacokinetics, *in vivo* distribution and tumor accumulation of liposomal drugs were systemically investigated. It was found that the higher serum stability and longer circulation time was successfully achieved by the crosslinking in the liposomal bilayers post UV irradiation. Also, the *in vitro* and *in vivo* tumor suppressing efficacy of 5-Fu was significantly promoted by the cooperative effects of EPR effect and temperature as well as Fab moiety. All the experimental results clearly demonstrated that the contradiction between particle stability and sufficient drug release

was successfully solved by using this novel thermoresponsive immunoliposomal drug delivery system, which merits further investigation for pre-clinical experiments and clinical trials.

Acknowledgements

This research was supported by National Science Foundation of China (81372330，81372312，81201584，81402454, 31400778); Shanghai Science and Technology Committee (12ZR1439800, 12ZR1454200, 12431900802, 14ZD1900403); Foundation of PLA (13QNT104) and Youth fund of the Second Military Medical University (2013QN14).

References:

1. Rosano L., Cianfrocca R., Tocci P., Spinella F., Di Castro V., Caprara V., Semprucci E., Ferrandina G., Natali P. G., Bagnato A. Cancer Res. 2014;

2. Kutty R. V., Wei Leong DT, Feng S. S. Nanomedicine (Lond). 2014;9(5):561-564.

3. Jang S. H., Wientjes M. G., Lu D., Au J. L. Pharm Res. 2003;20(9):1337-1350.

4. Jain R. K. J Natl Cancer Inst. 1989;81(8):570-576.

5. Wu C., Li H., Zhao H., Zhang W., Chen Y., Yue Z., Lu Q., Wan Y., Tian X., Deng A. Nanoscale Res Lett. 2014;9(1):447.

6. Markman J. L., Rekechenetskiy A., Holler E., Ljubimova J. Y. Adv Drug Deliv Rev. 2013;65(13-14):1866-1879.

7. Au J. L., Jang S. H., Zheng J., Chen C. T., Song S., Hu L., Wientjes M. G. J Control Release. 2001;74(1-3):31-46.

8. Kutty R. V., Feng S. S. Biomaterials. 2013;34(38):10160-10171.

9. Maeda H. J Control Release. 2012;164(2):138-144.

10. Iyer A. K., Khaled G., Fang J., Maeda H. Drug Discov Today. 2006;11(17-18):812-818.

11. Kano M. R., Bae Y., Iwata C., Morishita Y., Yashiro M., Oka M., Fujii T., Komuro A., Kiyono K., Kaminishi M., Hirakawa K., Ouchi Y., Nishiyama N., Kataoka K., Miyazono K. Proc Natl Acad Sci U S A. 2007;104(9):3460-3465.

12. Hyde S. C., Emsley P., Hartshorn M. J., Mimmack M. M., Gileadi U., Pearce S. R., Gallagher M. P., Gill D. R., Hubbard R. E., Higgins C. F. Nature. 1990;346(6282):362-365.

13. Ambudkar S. V., Kim I. W., Sauna Z. E. Eur J Pharm Sci. 2006;27(5):392-400.

14. Barenholz Y. J Control Release. 2012;160(2):117-134.

15. Saif M. W. JOP. 2013;14(6):686-688.

16. Li W., Zhao H., Qian W., Li H., Zhang L., Ye Z., Zhang G., Xia M., Li J., Gao J., Li B., Kou G., Dai J., Wang H., Guo Y. Biomaterials. 2012;33(21):5349-5362.

17. Ulbrich K., Subr V. Adv Drug Deliv Rev. 2004;56(7):1023-1050.

18. Kneidl B., Peller M., Winter G., Lindner L. H., Hossann M. Int J Nanomedicine. 2014;9(4387-4398.

19. Li W., Zhao M., Ke C., Zhang G., Zhang L., Li H., Zhang F., Sun Y., Dai J., Wang H., Guo Y. Biomed Res Int. 2013;2013(305089.

20. Li W., Li H., Li J., Wang H., Zhao H., Zhang L., Xia Y., Ye Z., Gao J., Dai J., Wang H., Guo Y. Int J Nanomedicine. 2012;7(4661-4677.

21. Temprana C. F., Duarte E. L., Taira M. C., Lamy M. T., Del Valle Alonso S. Langmuir. 2010;26(12):10084-10092.

22. Ciccolini J., Mercier C., Blachon M. F., Favre R., Durand A., Lacarelle B. J Clin Pharm Ther. 2004;29(4):307-315.

23. Wrightson W. R., Myers S. R., Galandiuk S. Biochem Biophys Res Commun. 1995;216(3):808-813.

24. Tuscano J. M., Martin S. M., Ma Y., Zamboni W., O'Donnell R. T. Clin Cancer Res. 2010;16(10):2760-2768.

25. Zhang Y., Huo M., Zhou J., Xie S. Comput Methods Programs Biomed. 2010;99(3):306-314.

26. Oba M., Miyata K., Osada K., Christie R. J., Sanjoh M., Li W., Fukushima S., Ishii T., Kano M. R., Nishiyama N., Koyama H., Kataoka K. Biomaterials. 2011;32(2):652-663.

27. Akimoto J., Nakayama M., Sakai K., Okano T. Biomacromolecules. 2009;10(6):1331-1336.

28. Tredan O., Galmarini C. M., Patel K., Tannock I. F. J Natl Cancer Inst. 2007;99(19):1441-1454.

29. Hanahan D., Weinberg R. A. Cell. 2000;100(1):57-70.

30. Hanahan D., Weinberg R. A. Cell. 2011;144(5):646-674.

31. Li W., Li J., Gao J., Li B., Xia Y., Meng Y., Yu Y., Chen H., Dai J., Wang H., Guo Y. Biomaterials. 2011;32(15):3832-3844.

32. Kneidl B., Peller M., Winter G., Lindner L. H., Hossann M. Int J Nanomedicine. 2014;9(4387-4398.

33. Wu Y., Yao J., Zhou J., Dahmani F. Z. Int J Nanomedicine. 2013;8(3587-3601.

34. van Elk M., Deckers R., Oerlemans C., Shi Y., Storm G., Vermonden T., Hennink W. E. Biomacromolecules. 2014;15(3):1002-1009.

35. Mussi S. V., Sawant R., Perche F., Oliveira M. C., Azevedo R. B., Ferreira L. A., Torchilin V. P. Pharm Res. 2014;31(8):1882-1892.

36. Akiyama Y., Kikuchi A., Yamato M., Okano T. Langmuir. 2004;20(13):5506-5511.

37. Wu Y., Yang Y., Zhang F. C., Wu C., Lu W. L., Mei X. G. J Liposome Res. 2011;21(3):221-228.

Figure captions:

Figure 1: (a) Synthesis of PID 118-b-PLA71 diblock copolymers (PPDC). (b) Fabrication of Fab conjugated thermoresponsive liposomes (FCTRL). (c) Size distribution of irrad and non-irrad FCTRLs. (d) Schematic diagram of irrad and non-irrad liposomes. (e) The thermosensitive behavior of the PNIPAM and FCTRLs determined by the transmittance profile of the reflected in their volume phase transition temperature (VPTT). (f) The TEM morphology of FCTRLs at T>VPTT (left and middle panel) and T<VPTT (right panel). Scale bar: left 0.5μm, middle 200nm, right 0.5μm.

Figure 2: (a) Confirmation of Fab conjugation on the liposomal by CLSM. The Her-2 positive MDA-MB-231 cells were successively incubated with FCTRL and Alexa-Fluor 488 labeled Goat-anti-human secondary antibodies. The green color surrounding cells was observed by CLSM in both 2D and 3D models. Scale bar: 10μm. (b) Drug release profile of liposomal 5-Fu at 37 and 40℃. (c) The cytotoxicity profile of the empty FCTRLs and BCTRLs incubated with Her-2 positive MDA-MB-231 cells.

Figure 3: The effects of temperature and Fab on the intracellular uptake of liposomal Qds in MDA-MB-231 (a) and MCF-7 (c) cells indicated by the inverse fluorescent microscopy. Red fluorescence represents the intracellular Qds. Magnification times:20×20. The effects of temperature and Fab on the intracellular uptake of liposomal Qds in MDA-MB-231 (b) and MCF-7 (d) cells indicated by FCM. Data are mead ± SD (n=3).

Figure 4: Concentration dependent cytotoxicity evaluation of free and liposomal 5-Fu in MDA-MB-231 cells (a) and MCF-7 cells (d). Time dependent cytotoxicity evaluation of free and liposomal 5-Fu in MDA-MB-231 cells (b) and

MCF-7 cells (e). The IC50 to MDA-MB-231 (c) and MCF-7 (f) cells of free and liposomal5-Fu. Data are mead ± SD (n=3)

Figure 5: (a) *In vivo* distribution profile of frozen section from MDA-MB-231 bearing BAL B/C nude mice treated with free and liposomal FITC for 24 hours as visualized by CLSM, the green fluorescence represents the tumor accumulation and retention of FITC. Scale bar: 100µm. (b) MDA-MB-231bearing BAL B/C nude mice were treated with free and liposomal FITC, after 24 hours, mice were euthanized and organs were harvested, washed, and the FITC was extracted and quantified. Data are mean±SEM of four separate mice in each grou. (c-d) *In vivo* anticancer therapeutic effects in MDA-MB-231 (c) and MCF-7 (d) bearing BAL B/C nude mice after the first intravenous administration of PBS, free and liposomal 5-Fu. Data are mean±SD of 5 separate mice in each group.

Supplementary Figure 1: Time-concentration curve of free and liposomal 5-Fu in IRC mice by PK software.

Supplementary Figure 2: Schematic representation of temperature-triggered drug release from FCTRLs

Table 1: Serum Stability of the 5-Fu loaded immunoliposomes

Time (h)	Non-irrad		Irrad	
	Raduis (nm)	PDI	Radius (nm)	PDI
0	130.17±24.76	0.036	93.74±15.33	0.027
8	166.72±40.82	0.060	97.76±20.3	0.043
24	187.34±59.82	0.102	102.55±22.7	0.050

PDI: Polydispersity index

Table 2. Serum pharmacokinetic parameters comparing free and liposomal drugs.

Parameter	Unit	Free ADR	Non-irrad	Irrad
$t_{1/2}\alpha$	h	0.20±0.01	0.19±0.03	0.22±0.07
$t_{1/2}\beta$	h	0.98±0.18	3.83±0.78	2.24±2.21
$t_{1/2}\gamma$	h	8,63±3.83	21.63±0.60	34.59±1.29
CL	ml/h	9.74±1.71	1.47±0.10	0.65±0.07
C_{max}	μg/ml	55.05±7.98	57.83±2.55	58.17±5.23
AUC_{0-t}	(μg/ml)·h	85.49±15.1	455.17±34.85	787.12±94.01
MRT	h	5.74±1.96	28.03±0.69	49.16±1.87

$t_{1/2}$: the elimination half time

CL: clearance

C_{max}: the maximum observed concentration in the plasma

AUC: area under the concentration-time curve

MRT: mean residence time

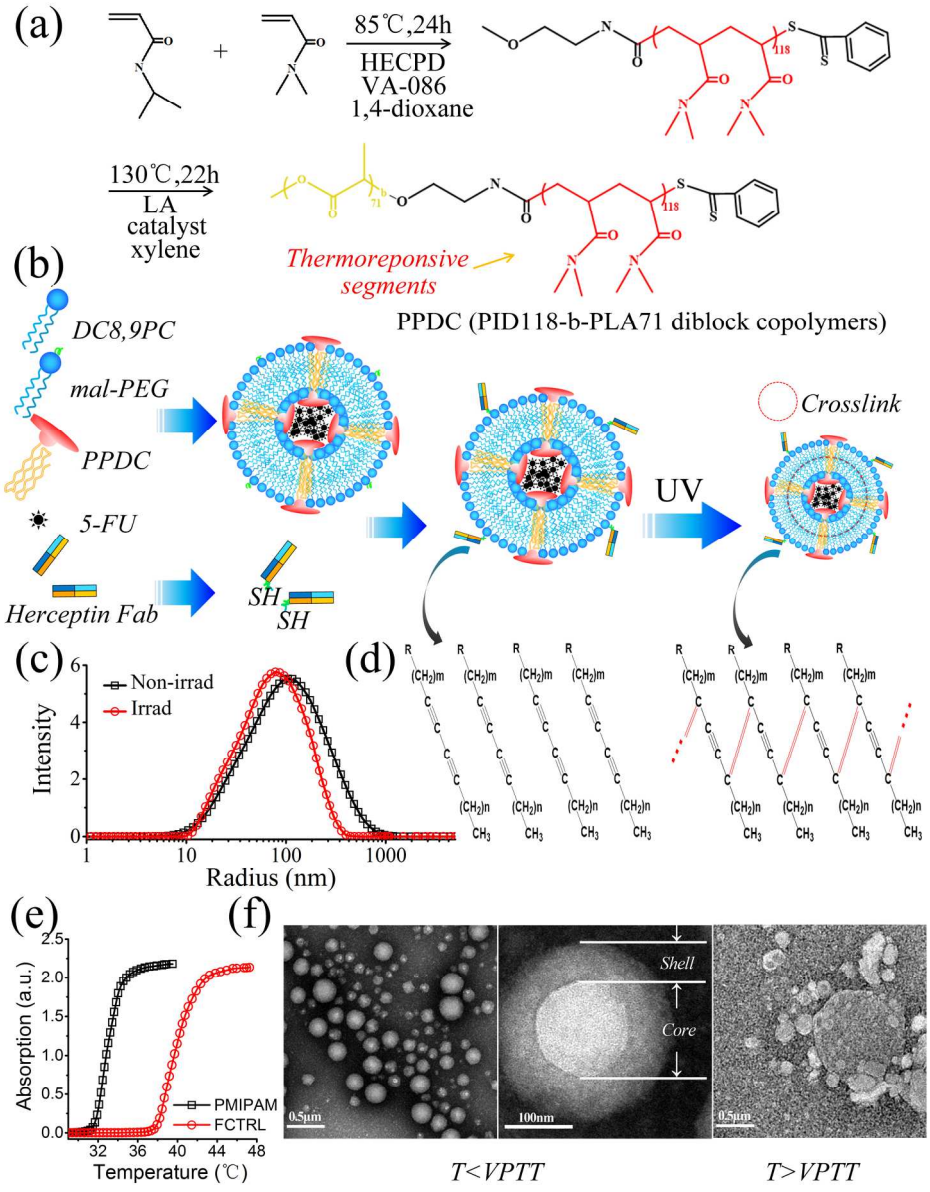

Figure 1: (a) Synthesis of PID 118-b-PLA71 diblock copolymers (PPDC). (b) Fabrication of Fab conjugated thermoresponsive liposomes (FCTRL). (c) Size distribution of irrad and non-irrad FCTRLs. (d) Schematic diagram of irrad and non-irrad liposomes. (e) The thermosensitive behavior of the PNIPAM and FCTRLs determined by the transmittance profile of the reflected in their volume phase transition temperature (VPTT). (f) The TEM morphology of FCTRLs at T>VPTT (left and middle panel) and T<VPTT (right panel). Scale bar: left 0.5μm, middle 200nm, right 0.5μm.
176x227mm (300 x 300 DPI)

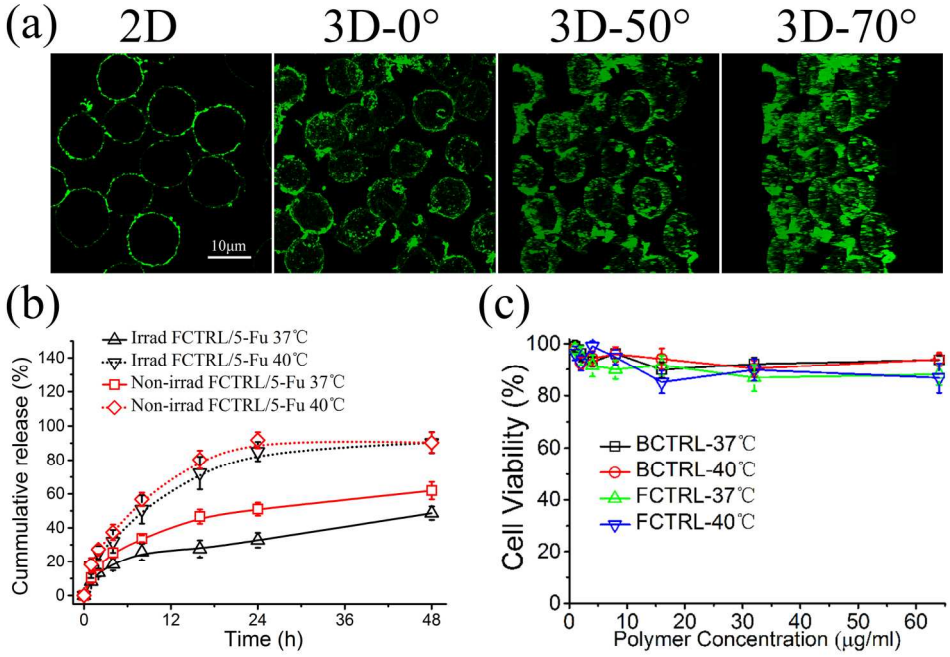

Figure 2: (a) Confirmation of Fab conjugation on the liposomal by CLSM. The Her-2 positive MDA-MB-231 cells were successively incubated with FCTRL and Alexa-Fluor 488 labeled Goat-anti-human secondary antibodies. The green color surrounding cells was observed by CLSM in both 2D and 3D models. Scale bar: 10μm. (b) Drug release profile of liposomal 5-Fu at 37 and 40℃. (c) The cytotoxicity profile of the empty FCTRLs and BCTRLs incubated with Her-2 positive MDA-MB-231 cells.
176x119mm (300 x 300 DPI)

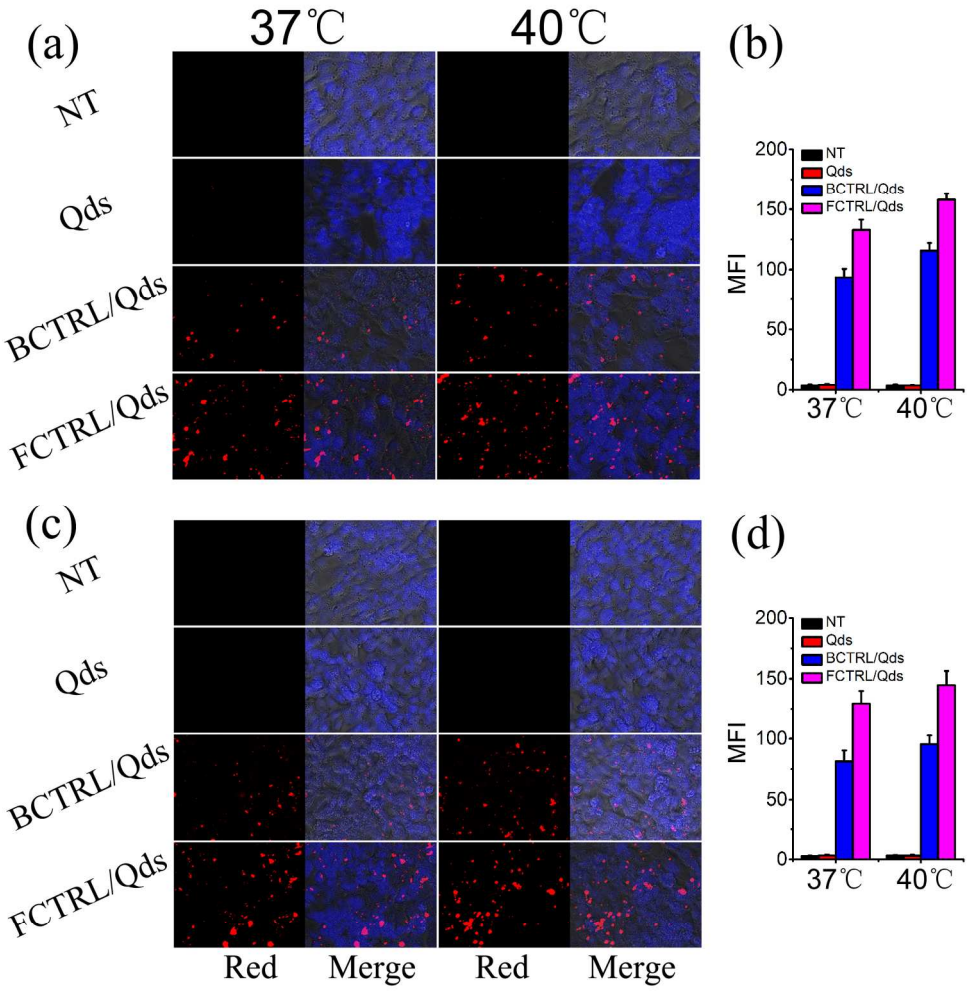

Figure 3: The effects of temperature and Fab on the intracellular uptake of liposomal Qds in MDA-MB-231 (a) and MCF-7 (c) cells indicated by the inverse fluorescent microscopy. Red fluorescence represents the intracellular Qds. Magnification times:20×20. The effects of temperature and Fab on the intracellular uptake of liposomal Qds in MDA-MB-231 (b) and MCF-7 (d) cells indicated by FCM. Data are mead ± SD (n=3). 176x183mm (300 x 300 DPI)

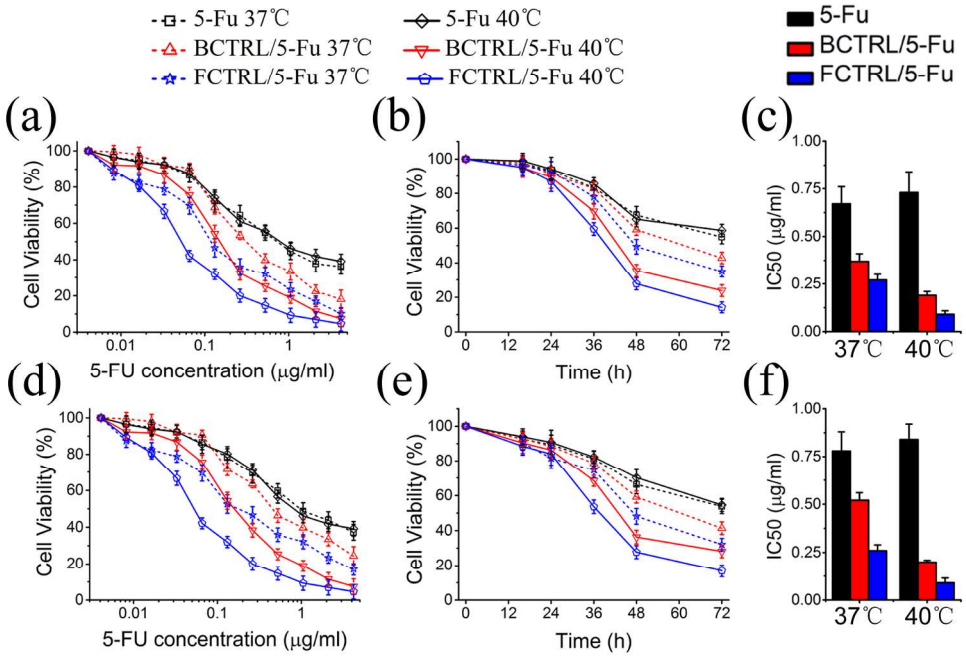

Figure 4: Concentration dependent cytotoxicity evaluation of free and liposomal 5-Fu in MDA-MB-231 cells (a) and MCF-7 cells (d). Time dependent cytotoxicity evaluation of free and liposomal 5-Fu in MDA-MB-231 cells (b) and MCF-7 cells (e). The IC50 to MDA-MB-231 (c) and MCF-7 (f) cells of free and liposomal5-Fu. Data are mead ± SD (n=3)
176x120mm (300 x 300 DPI)

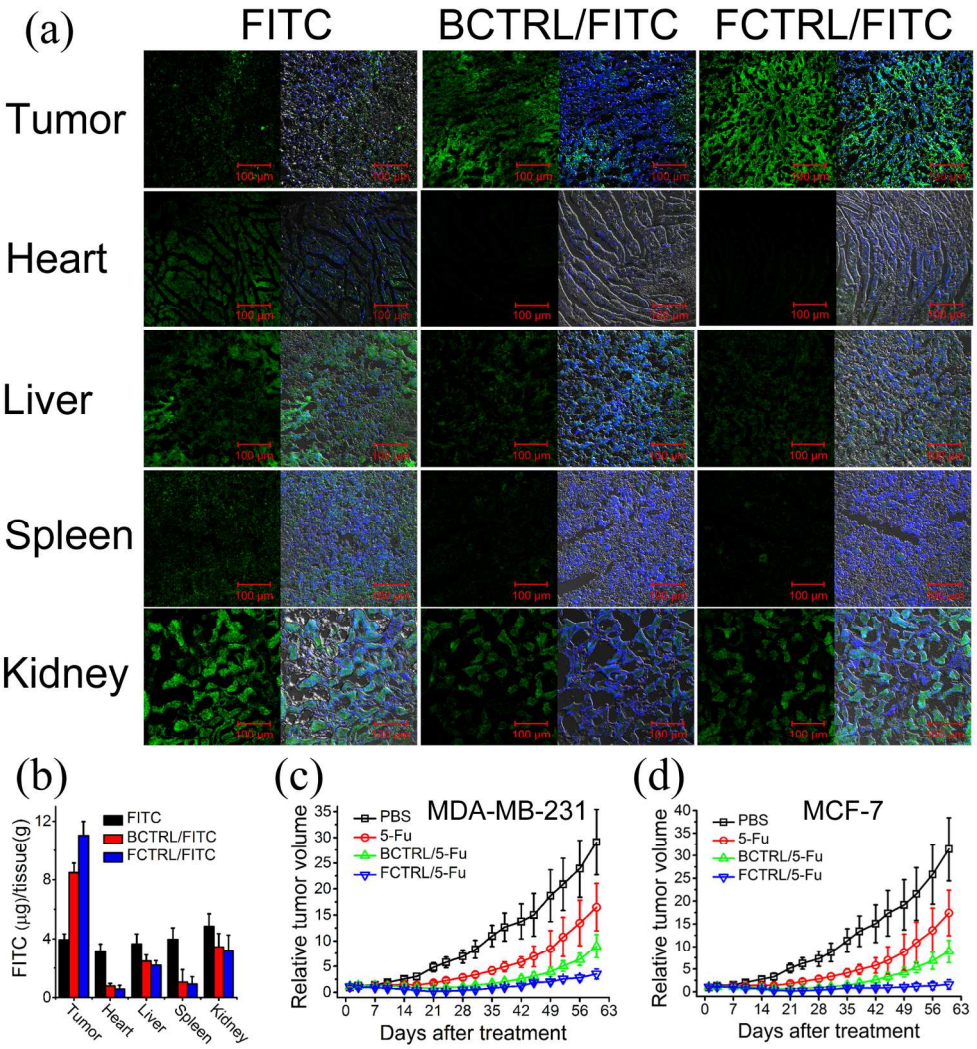

Figure 5: (a) In vivo distribution profile of frozen section from MDA-MB-231 bearing BAL B/C nude mice treated with free and liposomal FITC for 24 hours as visualized by CLSM, the green fluorescence represents the tumor accumulation and retention of FITC. Scale bar: 100μm. (b) MDA-MB-231bearing BAL B/C nude mice were treated with free and liposomal FITC, after 24 hours, mice were euthanized and organs were harvested, washed, and the FITC was extracted and quantified. Data are mean±SEM of four separate mice in each grou. (c-d) In vivo anticancer therapeutic effects in MDA-MB-231 (c) and MCF-7 (d) bearing BAL B/C nude mice after the first intravenous administration of PBS, free and liposomal 5-Fu. Data are mean±SD of 5 separate mice in each group.
185x198mm (300 x 300 DPI)

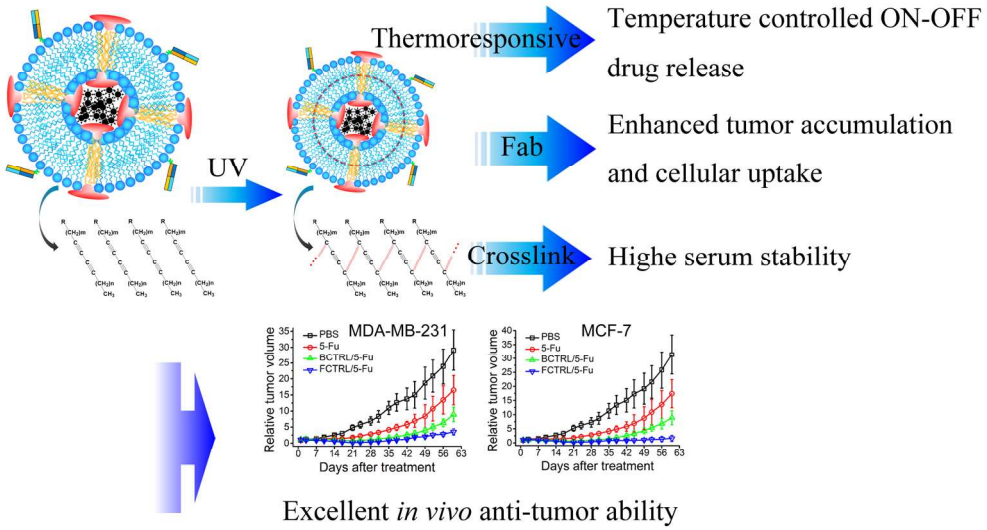

176x99mm (300 x 300 DPI)